

Excitons bound to Te isoelectronic dyads in ZnSeS. Marcet,¹ R. André,² and S. Francoeur^{1,*}¹*Département de Génie Physique, École Polytechnique de Montréal, Montréal, Québec, Canada H3C 3A7*²*Nanophysics and Semiconductor Group, Institut Néel, CEA/CNRS/Université Joseph Fourier,**25 rue des Martyrs, 38042 Grenoble, France*

(Received 11 October 2010; published 6 December 2010)

We report on the excitonic photoluminescence from individual Te dyads in ZnSe. Based on the emission characteristics of these pairs of pseudodonor impurities, we identify dyads of C_{2v} symmetry and determine their orientation with respect to the host lattice. The diamagnetic shift of the exciton indicates that the hole bound to the dyad is extremely localized. Measurements of large number of individual dyads reveal that (1) light-hole transitions located at higher energy are strongly suppressed, (2) the line shape of the observed phonon replica allows probing the phonon density of states, (3) dyads of various interatomic separations are observed, (4) the emission energy is extremely sensitive to the local environment of the dyad, and (5) dynamic variations in this local environment results in the intensity fluctuations and spectral diffusion.

DOI: [10.1103/PhysRevB.82.235309](https://doi.org/10.1103/PhysRevB.82.235309)

PACS number(s): 78.67.-n, 71.35.-y, 73.21.-b

I. INTRODUCTION

The interest in quantum dots stems from the control tridimensional confinement provides over electronic states and optical processes. This control, enhanced by our ability to vary the size, the composition and symmetry of quantum dots, has led to a number of seminal demonstrations in the fields of device applications,^{1,2} quantum information,^{3,4} single photon emission,⁵⁻⁷ and generation of entangled photons.^{8,9} However, full control over the response or behavior of quantum dots is impeded by the lack of control over processes by which quantum dots are formed. Self-assembled objects composed of 10^3 – 10^6 atoms are naturally associated to an important inhomogeneous broadening caused by various types of disorder. For example, it is statistically unlikely to fabricate a series of identical quantum dots for efficient laser operation, it is necessary to manually select quantum dots and temperature tune their emission to match it with a resonant cavity.¹⁰ It is also remarkably challenging to find quantum dots exhibiting a symmetry high enough to generate entangled photons via a biexcitonic cascade.^{8,9}

It has been recently demonstrated that single isoelectronic centers of one or two atoms can be optically resolved and individually studied.¹¹⁻¹⁴ First studied a few decades ago, these systems offer a number of advantageous characteristics over larger quantum dots. These quantum emitters are composed of one, two, or three isoelectronic traps whose positions are determined by the host lattice. Measured from a large ensemble, the inhomogeneous broadening, associated with distinct atomic configurations, i.e., different numbers of atoms or interatomic separation, is very large. It is then easy to identify and distinguish various configurations and even allows tuning the emission over a wide energy range.

However, the inhomogeneous broadening associated to an ensemble measurement of any given configuration is typically very small, the positions of atoms being rigidly set by the host lattice, and can approach the natural linewidth.¹⁵ Furthermore, in contrast to larger quantum dots, an isoelectronic center composed of only a few atoms will exhibit a well-defined symmetry set by the position of the constituent

atoms in the host lattice, allowing to create quantum emitters of various symmetries and study a series of subtle but interesting effects otherwise lost in larger dots of low or ill-defined symmetry.

More specifically, isoelectronic traps, or more precisely isovalent impurities forming excitonic bound states, allow forming various molecular states in a crystal and could become an interesting alternative to conventional quantum dots. Individual substitutional impurities such as N or Bi in, for example, GaP both bind excitons. The binding mechanisms most commonly accepted is the following.^{15,16} Isovalent substitution always creates a localized singularity in the host electronic density but it is generally not strong enough to localize charge carriers. However, if the electronegativity difference, this singularity can trap an itinerant carrier whose charge can be determined from simple considerations. Nitrogen, a pseudoacceptor, attracts and traps an electron while bismuth, a pseudodonor, traps a hole. This primary particle, tightly localized in a volume which is about the size of a unit cell,^{16,17} then binds a particle of the opposite charge through Coulomb interaction, resulting in a bound exciton. As opposed to the potential created by charged impurities, the potential trapping the primary particle is not coulombic and exhibit a much shorter range. This localization creates a fairly delocalized state in momentum space, explaining its deep level like behavior despite a binding energy that can be lower than that of hydrogenic impurities. Pairs of nearby isoelectronic centers bind exciton through the same mechanisms and, since the available interatomic separations largely determines the overall binding energy, a series of discrete emission, corresponding to different dyad configurations, are observed.¹⁵ Naturally, the binding energy is further enhanced by adding more atoms.¹⁸

A number of isoelectronic centers have been identified and studied in a number of semiconductor hosts. In this work, we analyzed the excitonic emission from Te dyads in ZnSe. After a description of a few practical aspects related to the sample studied and the measurement technique, we first describe results from macrophotoluminescence (PL) measurements. Then, we discuss in details a number of results

obtained by studying the photoluminescence of single Te dyads.

II. SAMPLE AND EXPERIMENTAL DETAILS

The sample investigated, grown by molecular-beam epitaxy on a GaAs substrate, consists of a single Te-doped layer inserted between two 40-nm-thick ZnSe layers. The nominal Te concentration was estimated from the ratio between the Te and Se fluxes impinging on the substrate. The ZnSe growth rate was calibrated at 0.5 monolayer (ML)/s by reflection high-energy electron diffraction oscillation. Tellurium was inserted during about 2 s with an equivalent flux of $\sim 2 \times 10^{-4}$ ZnTe ML/s. Such a low growth rate cannot be directly measured: the ZnTe growth rate (Te limited) was first calibrated at 0.1 ML/s and then the Te effusion cell was cool down following the Arrhenius law for Te sublimation to obtain the required Te flux. Finally the expected density of Te atom is $2500 \mu\text{m}^{-2}$. It corresponds to a dyad concentration of $4 \mu\text{m}^{-2}$ whose optical emission can be easily resolved by diffraction limited techniques.

Macrophotoluminescence measurements presented in Sec. III were performed at 12 K using an excitation wavelength of 405 nm. The microphotoluminescence measurements presented in the following sections were performed at 4.5 K in a custom-made confocal microscope in which the sample positioners and the microscope objective are located inside a liquid helium cryostat while the remaining optics are located outside at its top.¹⁹ A 405 nm excitation beam is brought to the microscope with a polarization-maintaining single mode optical fiber. In the microscope itself, the collimated beam is directed inside the cryostat through a reflection by a polarizing beamsplitter cube. It then passes through a motorized half wave plate and is focused on the surface of the sample using an aspherical lens. The excitation power is 250 μeV . The PL is collected by the same objective, transmitted through both the wave plate and the polarizing beamsplitter cube, both of which allow analyzing the polarization of the emitted light. The PL is then coupled into a 5 μm core polarization maintaining single mode optical fiber acting as a confocal aperture. This microscope provides a spatial resolution of 0.82 μm , allowing to probe the PL from a single Te dyad. The PL is analyzed using a 55 cm spectrometer and a charge coupled device camera providing an overall spectral resolution of 300 μeV . The cryostat tail is inserted in the bore of a superconducting coil magnet providing a magnetic field up to 7 T in Faraday configuration.

III. PHOTOLUMINESCENCE FROM THE Te δ -DOPED EPI-LAYER AND THE ZnSe HOST

The emission energy of excitons bound to isolated Te atoms or to Te dyads of various interatomic separations has not been accurately determined. A number of studies on Te-doped ZnSe have been reported^{12,20–25} but the spectral assignment is often contradictory. For example, the emission around 2.61–2.77 eV has been assigned to individual Te atoms^{20–22} or Te dyads^{12,23–25} and the emission at 2.48–2.50 eV has been assigned to Te dyads^{20,24} or higher order

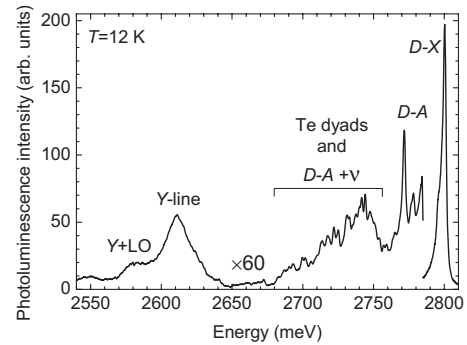


FIG. 1. Macrophotoluminescence of the δ -doped ZnSe sample. Donor bound excitons ($D-X$), donor-acceptor ($D-A$), and dislocation-related (Y) emission dominate the energy spectrum.

clusters.^{21,23} We note that in most of these studies little direct evidence is provided to support these assignments. Complicating matters further, the Te doping concentration typically exceeds 1%, resulting in broad emission lines instead of the sharp emission lines based on which assignments are typically proposed.^{26,27}

In this section, we present macrophotoluminescence measurements describing the emission from the host ZnSe crystal and identify the spectral regions where Te dyads were identified. Figure 1 shows the photoluminescence of the ZnSe:Te sample measured with an excitation area exceeding 500 μm^2 . Several features can be observed but none can be straightforwardly assigned to Te centers. The peak at 2.8 eV is assigned to excitons bound to donors ($D-X$) (Refs. 25 and 28) and the sharp lines between 2.76 and 2.85 eV are assigned to donor-acceptor pair emission ($D-A$).^{25,29} The emission line Y at 2.61 eV and its longitudinal optical (LO) phonon replica were assigned to Te dyads in Ref. 23 but this feature was observed in Te undoped samples and associated in Refs. 25 and 30 to the presence of dislocations. We therefore assume that this strong transition and its LO phonon replica are not related to the Te atoms.

A broad band exhibiting numerous sharp structures is observed between 2.68 and 2.76 meV. Almost all of the peaks located in this region can be assigned to LO, transversal optical, longitudinal acoustic, and transversal acoustic phonon replica and their combinations up to three phonons of the $D-A$ lines. We conclude that the ensemble measurement like the one presented in Fig. 1 on a δ -doped sample does not allow observing and identifying Te-related emission lines. In contrast, as has been reported recently¹² and as will be demonstrated in details in the following sections, micro-PL measurements reveal several distinct Te dyad configurations of different interatomic separations in the spectral range where phonon replica of the donor-acceptor transitions dominate ensemble measurements.

IV. LUMINESCENCE FROM SINGLE Te DYADS

In this section, we present the luminescence from single Te dyads, as microphotoluminescence provides advantageous conditions for the observation of Te related emission. Indeed, we find that the intensity from $D-A$ lines and their phonon

TABLE I. (Color online) Emission characteristics as a function of the point-group symmetry defined by the relative orientation of the two Te atoms in the anion sublattice. Optical transitions and their polarization are provided for different crystallographic orientations and defined with respect to the axes shown with respect to the Te molecule. x , y , and z represent linearly polarized singlets and (x,y) represent an unpolarized (np) degenerate doublet. The polarization angle is defined with respect to the $[110]$ direction in a plane whose normal is defined by wave vector of the emitted light, $[001]$.

Symmetry	Orientation ($a_0/2$)	Example ($n=1$)	Observation direction	Polarization direction		Polarization angle	
D_{2d}	$[n00]$ or $[0n0]$ $[00n]$		\bar{x} \bar{z}	y (x, y)	y, z (x, y)	45° np	$45^\circ, 135^\circ$ np
C_{3v}	$[nnn]$		$\bar{z} - \bar{y}$	$(x, y), (x, y)$	$(x, y), z$	np, np	$np, 0^\circ$
C_{2v}	$[nn0]$ $[n0n]$ or $[0nn]$		\bar{z} $\bar{y} + \bar{z}$	y, x y, x	x, y x, z, y	$0^\circ, 90^\circ$ $45^\circ, 135^\circ$	$90^\circ, 0^\circ$ $135^\circ, 45^\circ, 45^\circ$
C_2	$[310]$ $[420]$			3 transitions	4 transitions	26° or 116° 18° or 108°	26° or 116° 18° or 108°
C_s	$[211]$ $[411]$			3 transitions	4 transitions	18° or 108° 30° or 120°	18° or 108° 30° or 120°

replica varies considerably on the surface of the sample on a micron scale and the emission from Te centers, occurring at energies between 2690 and 2770 meV, can easily be observed and studied in regions of the sample where this unresolved emission is weak.

The nominal surface concentration of the δ -doped Te (001) plane is $2500 \mu\text{m}^{-2}$. Assuming a simple stochastic distribution of Te atoms, we estimate the surface concentration of dyads and triads at $4 \mu\text{m}^{-2}$ and $0.02 \mu\text{m}^{-2}$, respectively. Considering that the detection area is about $1 \mu\text{m}^2$, emission from isolated Te atoms should be unresolvable and the emission from Te triads should seldom be observed. Although a perfectly random distribution is unlikely, these relative concentrations nonetheless indicate that only Te dyads are in the appropriate range for single emitter spectroscopy. Indeed, from a large number of measurements, we estimated that the dyad surface concentration is about $1 \mu\text{m}^{-2}$, indicating that the deviation from a random distribution does not affect the argument presented above.

Measuring a single emitter lifts the orientational degeneracy¹¹ and allows the determination of symmetry of the dyad by a careful analysis of the number of emission lines observed and the orientation of their polarization maxima with respect to the crystal lattice.³¹ We begin by presenting an analysis of the excitonic structure for Te dyads. For isoelectronic dyads, in contrast to conventional quantum dots where strain and confinement push light-hole bands to high energy, the analysis includes both heavy- and light-hole bands. Hence, neglecting spin-orbit bands located 430 meV above,³² eight excitonic states are considered. Taking into account the effects of the electron-hole exchange interaction and the strain field produced by the Te centers and their neighboring atoms, the characteristics of excitonic spectra can be used to unambiguously determine the symmetry of the dyads.

Te being isovalent to Se, configurations and symmetries of dyads are determined by positions of substitutional Te atoms in the anion sublattice. Table I provides the number of

allowed transitions, their degeneracy and their polarization characteristics for dyads of various symmetries.³¹ Two scenarios exist for D_{2d} and C_{2v} symmetries, depending if the dyad direction is normal (called in plane) or not (out of plane) to the wave vector of the emitted light, $[001]$. This table allows an analysis of the excitonic structure under two scenarios. The first applies to strain free ZnSe in which heavy- and light-hole bands are degenerated and all excitonic states exhibit a strongly mixed character. The optical transitions and their respective polarization are given by the two columns under the headings *polarization direction* and *polarization angle*. For the considered point-group symmetries, optical transitions take either the form of linearly polarized singlets, x , y , or z , and nonpolarized (np) degenerate doublets, (x,y) . This scenario is usually the case for isoelectronic centers.^{15,33,34} The second scenario is the one commonly used to analyze the emission from nanostructures in which confinement and strain significantly lifts the degeneracy of the heavy- and light-hole bands, simplifying the analyses by allowing to consider two independent and separable hole subspaces. The first and second subdivision of the columns mentioned above give the optical transitions associated to heavy- and light-hole bands, respectively. For the case at hand, we have an intermediate scenario where heavy-hole valence bands of ZnSe, epitaxially strained to the host GaAs substrate, is pushed 12.6 meV below light-hole valence bands. Although significant compare to the exchange and crystal-field interaction, this valence-band splitting may not be large enough to decouple heavy- and light-hole excitonic states. Nonetheless, the mixing of the two hole subspaces is expected to be considerably reduced.

Before analyzing the experimental results, it is important to note that the symmetry of dyads presented in Table I does not take into account the tetragonal distortion of the ZnSe host induced by the GaAs substrate. Considering a host symmetry of D_{2d} instead of T_d significantly affects the overall symmetry of dyads. For example, out-of-plane C_{2v} becomes C_1 , C_{3v} becomes C_{1h} , in-plane D_{2d} becomes D_2 , and in-plane

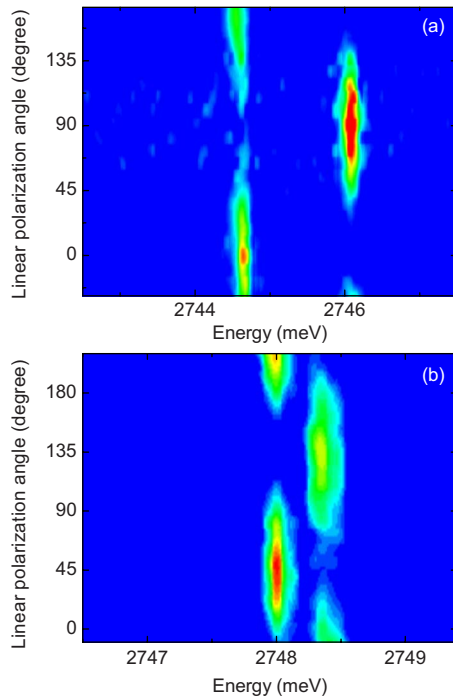


FIG. 2. (Color online) PL from single Te dyads where only transitions with a heavy-hole character are observed. (a) In-plane C_{2v} and (b) out-of-plane C_{2v} .

C_{2v} and out-of-plane D_{2d} remains unaffected. Although the symmetry is lowered by most forms of perturbations, it does not necessarily mean that its strength is sufficient enough to lift excitonic degeneracies and significantly mix excitonic states to increase the number of allowed transitions. It will be demonstrated in the next section that the excitonic emission of Te dyads in ZnSe can be adequately analyzed using the symmetry presented in Table I provided that the effects of strain, lifting the degeneracy of heavy- and light-hole bands, is taken into account. Furthermore, dyads of symmetry as low as C_{1h} and C_1 would produce an emission spectra composed of seven linearly polarized transitions. Since spectra presenting such characteristics have not been observed, it is assumed that the tetragonal distortion is not strong enough to significantly affect the effective symmetry of dyads and will be neglected in the following discussion.

Figure 2 presents the intensity of the luminescence from two distinct dyads as a function of the energy and polarization angle. Both spectra are composed of two linearly polarized transitions. The modest splitting between these two transitions (<2 meV) is much smaller than the valence band splitting expected from the ZnSe strained epilayer, about 12.6 meV,^{35,36} indicating that the observed excitonic states have either a dominant heavy- or light-hole character. The compressive strain implies that heavy-hole states are located at lower energy. A careful search at higher energy under various excitation powers did not reveal a second set of transitions associated with the light-hole states, indicating that thermalization to the lowest excitonic states is efficient, as generally observed at low temperature.

The symmetry of these two dyads can easily be determined from the data in Table I. Panel (a) shows two singlets

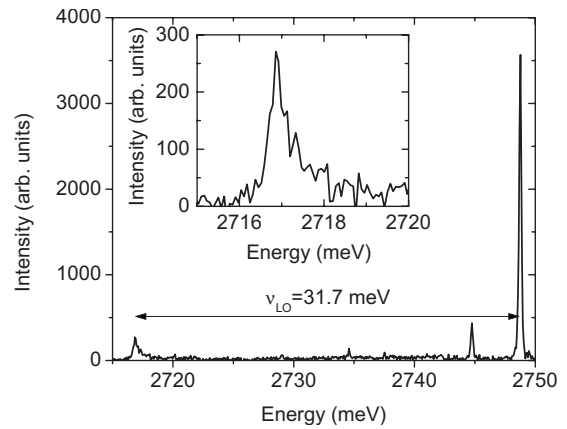


FIG. 3. PL intensity of a Te dyad for linear polarization at 135° . A LO phonon replica is observed on the low-energy side. The inset zooms on the phonon replica peak. The integration time is 30 s.

polarized along 0° and 90° . This signature is unambiguously associated with an in-plane dyad of C_{2v} symmetry, as it is the only one producing two heavy-hole singlets polarized along $[110]$ and $[\bar{1}\bar{1}0]$. The emission from the dyad presented in panel (b) is polarized along 45° and 135° . Table I indicates that the emission from in-plane D_{2d} dyads should be composed of one heavy-hole and two light-hole singlets and that the emission from out-of-plane C_{2v} dyads should be composed of two heavy-hole and three light-hole singlets, all polarized along 45° or 135° . The presence of two heavy-hole singlets strongly suggests that the symmetry of this dyad is also C_{2v} , but instead of being oriented perpendicular to the emission wave vector $[001]$, it is oriented at 45° . The identification of the symmetry of this second dyad was based on the assumption that there is no significant mixing of the heavy- and light-hole states. As mentioned, we expect a single heavy-hole singlets from an in-plane dyad of D_{2d} but a weak second orthogonally polarized singlet could appear in the case of a strong mixing. This possibility is ruled for two reasons. First, the splitting of ~ 12.6 meV implies that the strength of this mixing should be rather small. Second, the emission energies of the dyads presented in Fig. 2 are very similar, which would not be expected from dyads of different configuration.

Figure 3 shows a peak separated from the excitonic transition by about 31.7 meV, revealing a phonon replica involving a LO phonon. The intensity ratio gives a Huang-Rhys factor of $S=0.15$, much smaller than the value $S=1.1$ estimated from macroscopic measurements on δ -doped ZnSe:Te with relatively high Te concentration.²⁵ As a single dyad is observed, the shape of the phonon replica directly probe the phonon density of states. In fact, the significant increase in width of the phonon replica (full width at half maximum = 0.7 meV) compare to the zero-phonon line (0.15 meV, limited by the resolution of our setup) corresponds to the calculated phonon density of states (0.52 meV).³⁷ We can then assume that the asymmetrical shape of the phonon replica peak is related to the phonon density of state.

We measured the PL of the dyad shown on Fig. 2(b) under the influence of a magnetic field applied in Faraday configuration along the $[001]$ direction. Figure 4 shows the PL in-

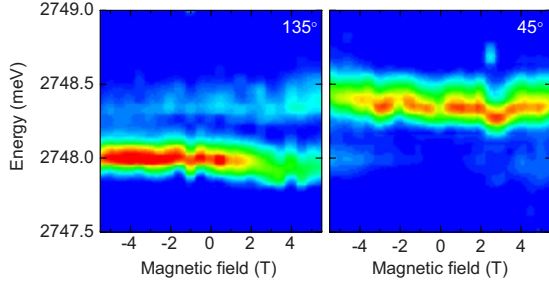


FIG. 4. (Color online) PL intensity (color scale) as a function of the emission energy and magnetic field for linear polarization at 45° and 135° .

tensity as a function of the emission energy and the magnetic field measured for polarization angles of 45° and 135° . For the signal polarized at 45° , effects related to intensity fluctuations and spectral diffusion will be discussed in Sec. VI. The intensity of the two transitions polarized at 135° varies asymmetrically as a function of the magnetic field. This asymmetry is not yet understood. The field induces a very small Zeeman splitting of $13 \pm 3 \mu\text{eV T}^{-1}$ and a small depolarization of both transitions. The diamagnetic shift common to both transitions, calculated with $\frac{1}{2}\sum_{i=1}^2 E_i(B) - E_i$, is quadratic with the magnetic field with a diamagnetic coefficient of $1.14 \pm 0.13 \mu\text{eV T}^{-2}$. This coefficient can be used to estimate the localization of the carriers of the exciton bound to the Te dyad. The diamagnetic shift coefficient of two confined particles without Coulomb interaction can be written as³⁸

$$\gamma = \frac{e^2}{8} \left(\frac{\langle r_e^2 \rangle}{m_e} + \frac{\langle r_h^2 \rangle}{m_h} \right) = \gamma_e + \gamma_h, \quad (1)$$

where m_h and m_e are the usual carrier effective masses and $\langle r_h^2 \rangle^{1/2}$ and $\langle r_e^2 \rangle^{1/2}$ are the average radii of the localization region of the hole and electron. Assuming it is bound to a hole of larger mass, the calculated radius of the electron wave function is about 3.25 nm. According to Eq. (1), the diamagnetic shift associated to the electron should then be $\gamma_e = 1.1 \mu\text{eV T}^{-2}$. Using the experimentally measured shift and an heavy-hole mass of $m_h = 0.6m_0$, the hole contribution is $\gamma_h < 0.17 \mu\text{eV T}^{-2}$ and its radius should then be less than 2.1 nm. Although an approximate value, it reveals a strong localization of the hole wave function, in agreement with the Hopfield-Thomas-Lynch (HTL) model for an isoelectronic pseudodonor.³⁹

V. DYAD CONFIGURATIONS

For nitrogen in GaP and GaAs, two of the most studied isoelectronic systems, dyad emission extends 130 and 160 meV below that of the exciton bound to a single nitrogen atom.^{15,27} The multiple dyad configurations, defined by the symmetry and interatomic separation, produce an emission spectra composed of several discrete lines. As the energy separation between dyads of different configurations is much larger than energy spanned by the excitonic states of any given one, it was relatively straightforward to deduce the

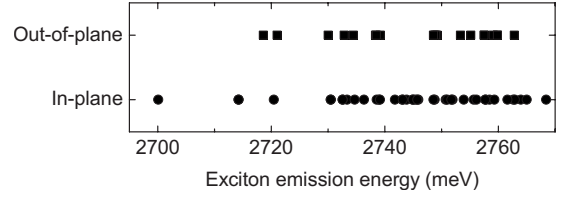


FIG. 5. Emission energy of all dyads observed in this work classified according to their orientation, in plane or out of plane.

configuration of the dyads based on the characteristics of their experimental spectra. In contrast, it is considerably more challenging to determine atomic configurations of Te dyads in ZnSe.

Emission from excitons bound to isolated Te atoms could not be observed or identified and could not therefore be used as a reference for the analysis of the configuration. Since the concentration of Te is relatively high, its emission should have been observed in both macroluminescence and microluminescence measurements, provided that its energy is located in the band gap of ZnSe. However, all spatially unresolved lines shown in Fig. 1 could readily be assigned to impurities commonly found in ZnSe. This may suggest that the Te bound excitonic state may be resonant with the valence band of ZnSe. This is the case for nitrogen atoms in GaAs where the excitonic state is located about 150 meV above the conduction-band minimum.²⁷

Figure 5 shows the emission energy of the excitonic transitions of all dyads observed and analyzed in this work. As had been previously reported,¹² we found that the emission from Te dyads produce a rich spectra spanning more than 70 meV in energy. We discuss in this section the origin of this wide distribution. We assume that Te atoms always occupy anionic sites as if a significant fraction of Te atoms had been interstitial, their emission spectra would have revealed a large number of dyads of relatively low symmetry.

The large variation in emission energies suggests that these dyads are likely composed of dyads of different configurations. However, we have analyzed the emission of a large number of dyads emitting over a wide energy range and we were unable to find dyads with a symmetry other than C_{2v} . More specifically, no dyads of C_{3v} and D_{2d} symmetries could be conclusively identified despite actively looking for their presence. However, this does not imply that all dyad observed share the same interatomic separation. Indeed, it has been established that the emission energy does not vary monotonically as a function of interatomic separation¹⁷ because of an elongation of the electron wave function along $\langle 110 \rangle$, the two lowest energy configuration correspond to dyads of first and fourth nearest anionic neighbor, both of C_{2v} symmetry. In GaAs, the two lowest energy nitrogen dyads are indeed of C_{2v} symmetry and are separated by 10 meV,¹¹ and, theoretically, a similar ordering has been found in GaP with a separation of about 40 meV.¹⁷ Therefore, it appears likely that first (TeTe₁) and fourth (TeTe₄) neighbors are observed. Furthermore, the large energy spread might suggest that other dyads, predominantly oriented along $\langle 110 \rangle$, might contribute to the data shown in Fig. 5.

Even if a large fraction of this energy spread can be explained by the presence of a number of dyads with different

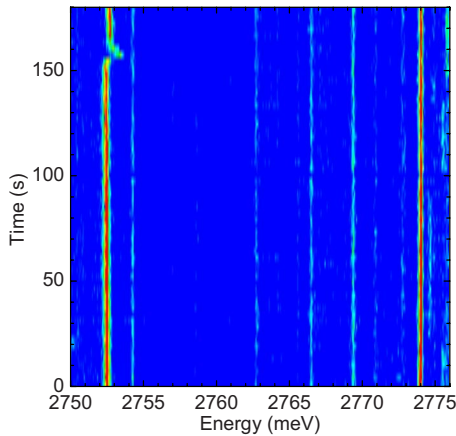


FIG. 6. (Color online) Time evolution of the energy and intensity of the luminescence for a few dyads located in the same detection volume. The integration time is 3 s and the linear polarization angle is 0° . The transition positioned at lower energy, associated to a single in-plane C_{2v} dyad, exhibits an abrupt change at around 150 s.

interatomic configuration, effects related to inhomogeneous broadening are also considerable. As mentioned above, it is impossible to group dyads with identical configurations. In contrast, inhomogeneous broadening of nitrogen dyads in GaAs is less than a few millielectron volts,¹¹ and much lower than the energy separation between different dyad configurations. The lack of obvious clustering of the data presented in Fig. 5 suggests that the broadening is similar in magnitude to the energy separation between configurations. This large inhomogeneous broadening could be explained by a number of factors. First, a dislocation-related emission (Y) was clearly identified from the macroluminescence spectra. This suggests that the crystal quality is somewhat compromised by the strain field created by the dislocation and the electric field possibly created by strings of trapped charges. This results in fluctuations in local environment on a scale that cannot be probed by diffraction limited techniques. Furthermore, Fig. 1 reveals the presence of a significant number of donors and acceptors and any dopants overlapping with the wave function of the Coulomb-bound electron will significantly affect the emission energy of the dyad.

It is important to reiterate that this inhomogeneous broadening is not related to the dyad itself but to a perturbation located in its immediate environment. Therefore, in principle, an immediate vicinity of better crystallinity and lower dopant concentration should offer the uniformity found in other isoelectronic systems.^{11,15}

VI. INTENSITY AND SPECTRAL FLUCTUATIONS

The emission from Te dyads often exhibits intensity fluctuations and spectral diffusion. These variations occur on a time scale spanning at least two orders of magnitude and appear to be sensitive to the level of excitation. Figure 6 shows the evolution of a spectrum as a function of time for a polarization angle of 0° . The line located on the low-energy side is emitted by an in-plane C_{2v} dyad. The other lines com-

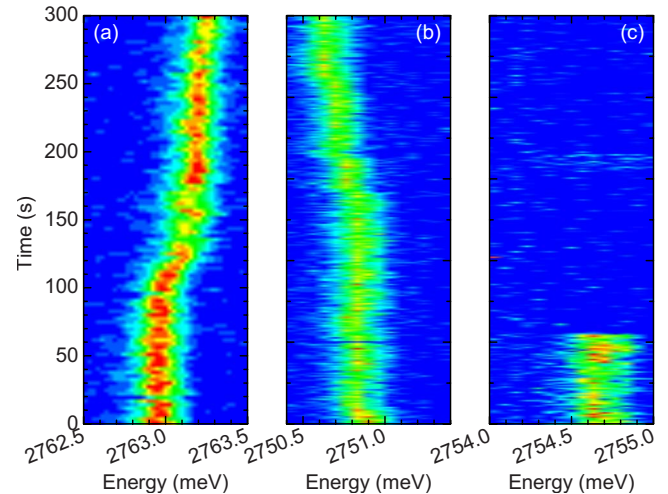


FIG. 7. (Color online) Time evolution of the emission spectra from three different dyads. The integration time is 0.1 s and the polarization angle is 0° . These spectra are representative of the various behaviors observed.

posing these spectra are emitted by three or more dyads located in the same detection volume. At around 150 s, a perturbation, lasting about 8–10 s, occurring only in the close vicinity of the C_{2v} dyad, blueshifts its energy by approximately 1 meV. The length scale of the perturbations at the origin of these fluctuations consistently appears to be much less than the size of the detection volume as most all other emission lines remained unaffected by this sudden perturbation. Although such spectral diffusion is often seen as a deleterious, it can be useful to discriminate the emission from a number of emitters located in the same detection volume.

The spectral diffusion can also take the form of slow drifts. Figure 7 shows the luminescence of three in-plane C_{2v} singlets as a function of time. Panels (a) and (b) show a significant blueshift and redshift occurring on a time scale of hundreds of second and panel (c) shows an abrupt quenching of the emission. The occurrence of these phenomena intensifies at high excitation intensity. All the data presented in the other sections of this work were taken under the lowest excitation possible to reduce the spectral diffusion and temporary quenching of the emission.

For conventional quantum dots, an abrupt shift of the emission is generally explained by the electric field produced by charges dynamically trapped in the vicinity⁴⁰ while a continuous tuning of the emission occurs when a large number of charges are trapped at larger distances. The magnitude and sign of this Stark shift results from two opposing effects.⁴¹ The electric field reduces the energy of both electron and hole states and this way contributes to a redshift of the emission. The field also decreases the overlap of electron and hole wave functions, reducing the Coulomb energy and thereby contributing to a blueshift. For Te dyads, it appears that these two effects are of similar magnitude as both redshift and blueshift can readily be observed, the net result likely determined by the local environment of the dyad. Finally, the quenching presented in panel (c) of Fig. 7 is abrupt and common at high excitation intensity. It appears that long-lived traps in the close vicinity of the dyad

significantly perturb the radiative process for extended periods.

VII. CONCLUSION

We have presented a thorough analysis of Te dyads in ZnSe. In microphotoluminescence experiments, excitons bound to dyads of C_{2v} symmetry with various interatomic separations are observed. The diamagnetic shift are consistent with the HTL bound exciton model with a relatively delocalized electron state and a more localized hole state. For

all dyads, excitonic states of light-hole character appear to be suppressed and the emission is dominated by transitions involving only heavy-hole states. An analysis of a large number of dyads shows that several interatomic separations are likely observed. These last two aspects indicate large variations in atomic environments significantly affecting the excitonic states, resulting in an inhomogeneous broadening of considerable magnitude. Dynamic variations in local environments result in intensity fluctuations and spectral diffusion of the emission spanning time scale extending by several orders of magnitude.

*sebastien.francoeur@polymtl.ca

- ¹V. I. Klimov, A. A. Mikhailovsky, S. Xu, A. Malko, J. A. Hollingsworth, J. A. Leatherdale, H.-J. Eisler, and M. G. Bawendi, *Science* **290**, 314 (2000).
- ²M. Bruchez, Jr., M. Moronne, P. Gin, S. Weiss, and A. P. Alivisatos, *Science* **281**, 2013 (1998).
- ³N. Gisin, G. Ribordy, W. Tittel, and H. Zbinden, *Rev. Mod. Phys.* **74**, 145 (2002).
- ⁴E. Knill, R. Laflamme, and G. J. Milburn, *Nature (London)* **409**, 46 (2001).
- ⁵P. Michler, A. Imamoglu, M. D. Mason, P. J. Carson, G. F. Strouse, and S. K. Buratto, *Nature (London)* **406**, 968 (2000).
- ⁶P. Michler, A. Kiraz, C. Becher, W. V. Schoenfeld, P. M. Petroff, L. Zhang, E. Hu, and A. Imamoglu, *Science* **290**, 2282 (2000).
- ⁷C. Santori, M. Pelton, G. Solomon, Y. Dale, and Y. Yamamoto, *Phys. Rev. Lett.* **86**, 1502 (2001).
- ⁸R. M. Stevenson, R. J. Young, P. Atkinson, K. Cooper, D. A. Ritchie, and A. J. Shields, *Nature (London)* **439**, 179 (2006).
- ⁹A. Mohan, M. Felici, P. Gallo, B. Dwir, A. Rudra, J. Faist, and E. Kapon, *Nat. Photonics* **4**, 302 (2010).
- ¹⁰J. P. Reithmaier, G. S. Ogonk, A. Lffler, S. K. C. Hofmann, S. R. Abd, L. V. Keldysh, V. D. Kulakovskii, T. L. Reinecke, and A. Forchel, *Nature (London)* **432**, 197 (2004).
- ¹¹S. Francoeur, J. F. Klem, and A. Mascarenhas, *Phys. Rev. Lett.* **93**, 067403 (2004).
- ¹²A. Muller, P. Bianucci, C. Piermarocchi, M. Fornari, I. C. Robin, R. André, and C. K. Shih, *Phys. Rev. B* **73**, 081306 (2006).
- ¹³C. Kurtz, S. Mayer, P. Zarda, and H. Weinfurter, *Phys. Rev. Lett.* **85**, 290 (2000).
- ¹⁴S. Strauf, P. Michler, M. Klude, D. Hommel, G. Bacher, and A. Forchel, *Phys. Rev. Lett.* **89**, 177403 (2002).
- ¹⁵D. G. Thomas and J. J. Hopfield, *Phys. Rev.* **150**, 680 (1966).
- ¹⁶R. A. Faulkner, *Phys. Rev.* **175**, 991 (1968).
- ¹⁷P. R. C. Kent and A. Zunger, *Phys. Rev. B* **64**, 115208 (2001).
- ¹⁸S. Francoeur, S. A. Nikishin, C. Jin, Y. Qiu, and H. Temkin, *Appl. Phys. Lett.* **75**, 1538 (1999).
- ¹⁹S. Marcet, C. Ouellet-Plamondon, and S. Francoeur, *Rev. Sci. Instrum.* **80**, 063101 (2009).
- ²⁰D. Lee, A. Mysyrowicz, A. V. Nurmikko, and B. J. Fitzpatrick, *Phys. Rev. Lett.* **58**, 1475 (1987).
- ²¹T. Yao, M. Kato, J. J. Davies, and H. Tanino, *J. Cryst. Growth* **86**, 552 (1990).
- ²²C. D. Lee, H. K. Kim, H. L. Park, C. H. Chung, and S. K. Chang, *J. Lumin.* **48-49**, 116 (1991).
- ²³I. L. Kuskovskiy, C. Tian, G. F. Neumark, J. E. Spanier, I. P. Herman, W.-C. Lin, S. P. Guo, and M. C. Tamargo, *Phys. Rev. B* **63**, 155205 (2001).
- ²⁴C. S. Yang, D. Y. Hong, C. Y. Lin, W. C. Chou, C. S. Ro, W. Y. Uen, W. H. Lan, and S. L. Tu, *J. Appl. Phys.* **83**, 2555 (1998).
- ²⁵M. Jo, Y. Hayashi, H. Kumano, and I. Suemune, *J. Appl. Phys.* **104**, 033531 (2008).
- ²⁶J. D. Cuthbert and D. G. Thomas, *Phys. Rev.* **154**, 763 (1967).
- ²⁷X. Liu, M.-E. Pistol, and L. Samuelson, *Phys. Rev. B* **42**, 7504 (1990).
- ²⁸R. Bhargava, *Properties of Wide Bandgap II-VI Semiconductors* (Inspect, London, 1997), pp. 138–139.
- ²⁹J. L. Merz, K. Nassau, and J. W. Shiever, *Phys. Rev. B* **8**, 1444 (1973).
- ³⁰J. Schreiber, U. Hilpert, L. Höring, L. Worschech, B. König, W. Ossau, A. Waag, and G. Landwehr, *Phys. Status Solidi B* **222**, 169 (2000).
- ³¹S. Francoeur and S. Marcet, *J. Appl. Phys.* **108**, 043710 (2010).
- ³²M. Cardona, *J. Appl. Phys.* **32**, 2151 (1961).
- ³³Q. X. Zhao and B. Monemar, *Phys. Rev. B* **38**, 1397 (1988).
- ³⁴S. Marcet, C. Ouellet-Plamondon, J. F. Klem, and S. Francoeur, *Phys. Rev. B* **80**, 245404 (2009).
- ³⁵Y. R. Lee, A. K. Ramdas, L. A. Kolodziejcki, and R. L. Gunshor, *Phys. Rev. B* **38**, 13143 (1988).
- ³⁶C. G. Hodgins and J. C. Irwin, *Phys. Status Solidi A* **28**, 647 (2006).
- ³⁷D. N. Talwar, M. Vandevyver, K. Kunc, and M. Zigone, *Phys. Rev. B* **24**, 741 (1981).
- ³⁸S. N. Walck and T. L. Reinecke, *Phys. Rev. B* **57**, 9088 (1998).
- ³⁹J. J. Hopfield, D. G. Thomas, and R. T. Lynch, *Phys. Rev. Lett.* **17**, 312 (1966).
- ⁴⁰H. D. Robinson and B. B. Goldberg, *Phys. Rev. B* **61**, R5086 (2000).
- ⁴¹T. Arakawa, Y. Kato, F. Sogawa, and Y. Arakawa, *Appl. Phys. Lett.* **70**, 646 (1997).